SMITHSONIAN INSTITUTION
ASTROPHYSICAL OBSERVATORY

Research in Space Science

SPECIAL REPORT

Number 224

ELEVATION DIFFERENCES ON MARS

Carl Sagan and James B. Pollack

October 10, 1966

CAMBRIDGE, MASSACHUSETTS 02138

SAO Special Report No. 224

ELEVATION DIFFERENCES ON MARS

Carl Sagan and James B. Pollack

Smithsonian Institution
Astrophysical Observatory
Cambridge, Massachusetts 02138

7-66-8

TABLE OF CONTENTS

LIST OF ILLUSTRATIONS

ELEVATION DIFFERENCES ON MARS[1]

Carl Sagan[2] and James B. Pollack[3]

I. INTRODUCTION

Apart from the polar caps, Mars is divided into so-called bright and dark areas. The bright areas have a visual albedo of some 15% and are colored a dull orange ochre. Temporary incursions of bright-area material into the nearby dark areas (see, e. g., Slipher, 1962), polarimetric observations (Dollfus, 1957), and infrared radiometry as a function of Martian local time (Sinton and Strong, 1960) all show the bright areas to be composed of finely pulverized material; for this reason they are usually described as deserts. The dark areas have a visual albedo lower by several percent, and to many recent observers (Kuiper, 1957) have a gray-orange tint — although early observers (see, e. g., Antoniadi, 1930) regularly reported vivid greens and other hues, which were sometimes attributed to biological activity on Mars.

The prevailing opinion of most observers of Mars, for almost a century, has been that the dark areas are lowlands and the bright areas highlands. The curious resulting implication that fine particles of dust are preferentially present in the highlands does not seem to have been generally remarked upon. At the turn of the century, observations were performed of orange-ochre material beyond the Martian terminator and above bright areas — evidently being struck obliquely by the Sun's

[1]This research was supported in part through Grant NGR-09-015-023 from the National Aeronautics and Space Administration.

[2]Harvard University and Smithsonian Astrophysical Observatory.

[3]Smithsonian Astrophysical Observatory and Harvard College Observatory.

rays. Although it was soon concluded that a dust cloud had been viewed (Lowell, 1906), a connection between bright areas and elevations seems to have been established. Dark areas at the limbs against a black background appear illusorily as depressions, another contributing factor to early views on the subject.

From his inability to detect reliably mountain peaks illuminated beyond the terminator (a common observation for the Moon), Lowell (1906) concluded that the maximum heights of Martian mountains were about 0.8 km. However, a modern revision of this calculation (Tombaugh, 1961) sets the upper limit at 8 km. Moreover, such calculations implicitly assume steep slopes; a major elevation with shallow slopes would escape detection by this technique (Russell, Dugan, and Stewart, 1945). Detection of elevations by the shadows they cast is even more difficult, especially if slopes are shallow. Elevations at the illuminated limb would not be detectable (even at favorable opposition) as a departure from sphericity unless the elevation were greater than the limiting resolution, or some 40 km high. Thus, very little can be determined about elevations by these more-or-less direct observations.

Such events as the seasonal darkening wave of the Martian dark areas have long been interpreted in terms of biological processes (Trouvelot, 1884; for a recent discussion, see Sagan, 1966). By terrestrial analogy one might expect the lowlands to be warmer than adjacent highlands, apart from any effects of albedo. If we believe there is a biological premium for relatively high temperatures on chilly Mars, we might be tempted to call the dark areas lowlands.

Related reasoning concerns apparent frost phenomena. Polar-cap material is observed left behind in certain locales during the seasonal

regression of the cap, or is observed to advance preferentially in certain locales during the seasonal equatorward extension of the caps. These locales are usually bright areas; and certain standard features of Martian cartography (e. g., the "Mountains of Mitchell") are deduced on these grounds alone (Slipher, 1962). It is also maintained (Slipher, 1962) that the frost deposits seen on the morning limb of Mars tend to be localized preferentially in bright areas. Tombaugh (1966) has recently summarized some of the results of his 35 years of visual observations of Mars. In his Plate 1, the preferential extension of the polar cap into such Martian bright areas as Hellas[4] and Argyre are clearly seen (similar observations were made by Lowell – see, e. g., Lowell (1908), figure facing p. 74). A related phenomenon is seen in the last stages of regression of the southern polar cap. The last remnant of the cap lies near 85° S. latitude, 40° longitude, and is distinctly displaced from the south pole. In the maps of Dollfus (1961), this locale is a bright area, while the south pole itself is dark. It has also been observed, since the time of Flammarion, that certain bright areas – e. g., Nix Olympica – have white clouds preferentially forming over them (Slipher, 1962; Dollfus, 1961). Some of these apparent condensation phenomena usually occur in summertime, and are sometimes explained in terms of the larger quantities of atmospheric water vapor then available due to the springtime vaporization of the polar cap (that the Martian atmosphere has a larger quantity of water vapor in summer is now known through the spectroscopic observations of R. Schorn et al. (1966)).

[4] An index of many Martian place names used in the present paper appears in the caption to Figure 3.

Both the biological argument and the apparent frost phenomena argument hinge on the assumption that areas at higher elevation are at lower temperatures, especially near midday. While such is surely the case for the Earth, it does not follow that it is also the case for Mars, as we now undertake to demonstrate.

2. ARE HIGHLANDS COLDER THAN LOWLANDS ON MARS?

The elevations of the Earthare cooler than the neighboring lowlands for three principal reasons: (1) a diminished atmospheric greenhouse effect, (2) the generally greater inclination of elevations to the Sun's rays, and (3) the adiabatic cooling of rising air. We discuss each of these factors in turn, in their Martian application.

2.1 Martian Greenhouse Effects

Calculations of the extent of the atmospheric greenhouse effect on Mars have been attempted in the past (Sagan, 1961; Ohring, Wen Tang, and DeSanto, 1962), but with values of the total pressure, CO_2 and H_2O abundances, and bolometric albedo that we now know to be incorrect. We can easily see, however, that any differential greenhouse effect must be small on Mars, because the overall greenhouse effect is small. With a bolometric albedo $A \simeq 0.29$ (de Vaucouleurs, 1964), the radiation equilibrium temperature of Mars — averaged seasonally and diurnally — is about 208° K. The disk-integrated microwave brightness temperature of Mars represents a somewhat different average. The diurnal, and possibly the seasonal, thermal waves are essentially damped at the effective emitting level for wavelengths longward of 3 cm. But since we always see a hemisphere of Mars centered near the subsolar point, the microwave brightness temperatures must be biased toward high temperatures. Therefore, the fact that these radio temperatures are never more than 10 K° hotter than the computed equilibrium temperature (see, e.g., Dent, Klein, and Allen, 1965) shows that the absolute greenhouse temperature increment is smaller than 10 K°. The differential contribution between elevations and depressions should therefore be at most a few K°. The sample calculation of Appendix A confirms this conclusion more directly.

On the Earth, in contrast, the total greenhouse effect is some 35 K°, and a differential effect approaching 10 K° is not out of the question.

2.2 Martian Slopes

The mean slope of an elevated and, especially, mountainous area can affect its temperature. The larger the slope the greater is the ratio of the total surface area of the elevated region to the area on a smooth sphere covering the same territory, and the greater the area over which the insolation is distributed. The sloping regions will therefore tend to have a lower mean temperature. Infrared radiation onto the elevations from adjacent inclines and lowlands will tend to reduce the temperature differences due to slope between elevations and depressions. Thus the temperature differences discussed here will be upper limits. The mechanism chiefly responsible for steep slopes on terrestrial mountains, namely water erosion, is certainly inoperative on contemporary Mars, because of the low partial and total pressures. Analysis of the radar Doppler spectra of Mars tends to confirm this view: the quasi-specular half-width is generally small, at least at 12.5-cm wavelength, and is not noticeably broader in bright areas than in dark areas (Sagan, Pollack, and Goldstein, 1966). The radar data at 12.5-cm wavelength imply general slopes and random facets with inclinations of only a few degrees (Sagan, Pollack, and Goldstein, 1966). If such inclinations, α, were preferentially present on highlands, the decrease in temperature amounts to $(1 - \cos^{1/4} \alpha)\, T_s \simeq (\alpha^2\, T_s/8)$, where T_s is the temperature of a nearby lowland surface normal to the Sun's rays. For $\alpha < 10°$ and $T_s \sim 240°K$, this difference is always less than 1 K°. On the Earth, in contrast, slopes of 45° are not uncommon in mountainous regions, leading to

temperature differences due to slopes of some 25 K°. Actual values will be less than this, because of infrared radiation from adjacent areas.

In the remainder of this discussion, the Martian highlands are considered to correspond roughly to terrestrial mountain ranges and continents, and not to isolated mountain peaks. Similarly, lowlands correspond to the bottoms of oceans and bays, rather than to the smaller scale interalpine valleys.

2.3 Martian Heat Exchange With Adiabatically Cooled Air

When parcels of air move from low altitudes to high, they adiabatically expand and cool, because of the reduced ambient pressure. By exchanging heat (both radiatively and conductively) with the high-altitude surface, such parcels cool the highlands. If the Martian atmosphere is at all dynamically similar to the terrestrial, the effective diffusivity, $\kappa = K/\rho c_p$, will be a pressure-independent quantity (Goody, 1966). The effective conductivity, K, for exchange between ground and atmosphere, is then proportional to the density, ρ, of the atmosphere. We can then immediately anticipate that such heat exchange is significantly less important on Mars than on Earth, because the density of the Martian atmosphere is only about 10^{-2} that of the Earth's; there is less atmosphere available for heat exchange.

In Appendix B we show that the cooling of highlands because of the expansion of rising air amounts to no more than a few tenths of a degree.

2.4 The Albedo Argument

From the preceding analysis and Appendices A and B, we conclude that there is no reason to expect a substantial daytime temperature difference (more than a few degrees) between highlands and lowlands, even if elevation differences ~ 12.5 km are commonplace. At night all temperatures will be below freezing – both in highlands and in lowlands – and will be determined in large part by the thermal inertia. Infrared radiometric measurements are in accord with this view. The dark areas have a daytime temperature about 8 K° higher than the bright areas (Sinton and Strong, 1960). With contemporary values (de Vaucouleurs, 1964) of the bright area bolometric albedo $\simeq 0.3$ and the dark areas bolometric albedo $\simeq 0.2$, and assuming equal infrared emissivities, a noontime temperature difference of about 10 K° between bright and dark areas is predicted. Thus the dark areas are warmer than the bright areas because they absorb more sunlight – and no major temperature differences due to elevation differences are permitted.

3. A REEXAMINATION OF FROST DEPOSITS

Let us now reexamine the classical arguments given at the beginning of this discussion. We first consider the location of the border of the polar caps during their springtime recession. The following discussion does not depend significantly on the composition of the polar caps, and the word "frost" will apply both to condensed water and to condensed CO_2. Some of the frost will vaporize in sunlight; but its removal is limited chiefly by vertical eddy and molecular diffusion and by horizontal advection. The relative rate of mass loss through vaporization per square centimeter is

$$\frac{1}{m}\frac{dm}{dt} = \frac{p\Delta z}{mg\tau} \propto \frac{\bar{v}p\Delta z}{m} \quad , \tag{1}$$

where m is the mass of frost per unit area, p(T) is the vapor pressure above the frost, Δz is the vertical height over which the vapor has been distributed by diffusion and winds, g is the acceleration due to gravity, and τ is the characteristic time for the vapor to move horizontally at mean velocity $\bar{v}$ a distance of 1 cm, and has dimensions of seconds per centimeter.

We now want to determine the dependence of each quantity after the proportionality sign in equation (1) on the total atmospheric pressure, P. There are two reasons for the wind velocity to be greater at low pressure than at high – as is the case on Earth. First, because of friction with the ground in the surface layers, the velocity increases with altitude. Second, for no sources or sinks, the equation of mass continuity becomes $\vec{\nabla} \cdot (\rho \vec{v}) = 0$. Consider a volume element whose walls are fit to the crest and to the bottom edge

of the highland (see Figure 1). Then, by the Gauss divergence theorem, $\int (\rho v)_n \, dz = \text{const.}$ The subscript indicates normal components. With shallow slopes $(\rho v)_n \simeq (\rho v)$. Taking $v = \bar{v}$, a mean velocity in vertical section, we find $P\bar{v} = \text{const}$, $\bar{v} \propto P^{-1}$. Since we are concerned with static and not dynamic pressures, we have used the mass continuity equation, rather than the Bernoulli principle.

The vapor pressure p(T) is independent of P and is a function of the temperature alone. If the polar cap is optically thick, the albedo over both bright and dark areas will be that of the frost deposit. If the caps are partially transparent, the net albedo of frost plus surface will be less at dark areas than at bright areas. Especially since no systematic variation of polar cap albedo with the albedo of the underlying surface has ever been reported, the albedo difference can correspond to a temperature difference of a few degrees at most, with a correspondingly small influence on dm/dt.

At the low pressures of Mars, it is unclear whether Δz is determined by molecular diffusion or by eddy diffusion. In the former case, $\Delta z \propto P^{-1/2}$; in the latter, Δz is inversely proportional to a power of P greater than 1/2. We conservatively adopt $\Delta z \propto P^{-1/2}$. The total mass of the frost deposit, m, depends on the abundance of condensable vapor in the atmosphere at the time of deposition. We anticipate $m \propto P$, approximately.

Collecting results, we then find

$$\frac{1}{m}\frac{dm}{dt} \propto p(T)\, P^{-5/2} \quad . \tag{2}$$

An elevation and a depression on Mars, differing in total ambient pressure by a factor of 2, but with the same rate of polar cap regression, would require a ratio of vapor pressures of a factor 5. This

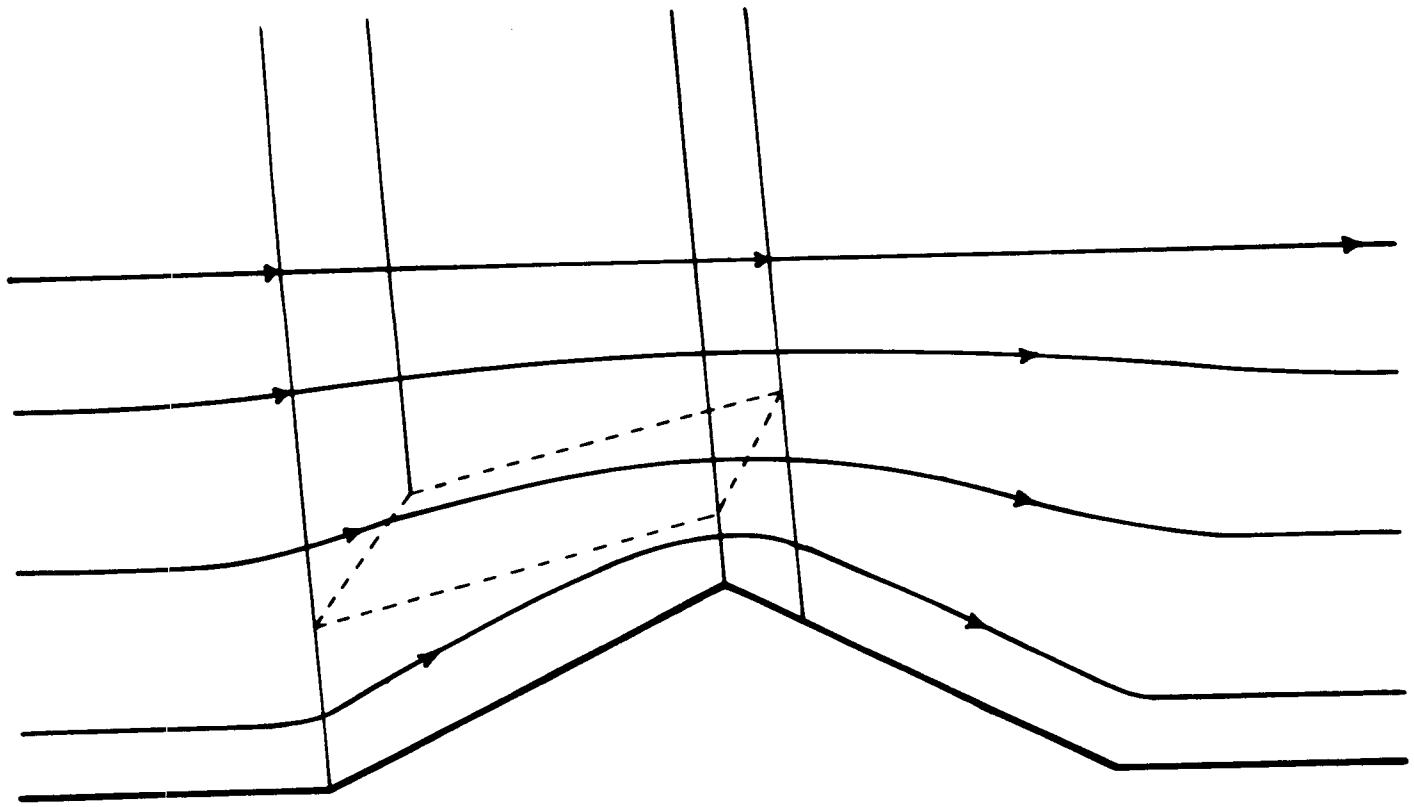

Figure 1. Schematic illustration of an elevation with atmospheric streamlines above. Fitted to the elevation is a Gaussian volume element (see discussion following equation (1)).

corresponds to a temperature difference between highland and lowland of 15 K° if the polar caps are H_2O (at ~ 240° K), or 12 K° if they are CO_2 [at ~ 140° K (Leighton and Murray, 1966)]. Such temperature differences exceed inadmissably the maximum temperature difference of a few degrees deduced at the polar cap from all causes, albedo differences included. Thus, equation (2) implies that where the total pressures are greater, the regression of frost deposits will be more sluggish. Hence, the preference of frost deposits for bright areas implies that bright areas are lowlands. On the Earth much larger temperature differences (and smaller pressure differences) between highlands and lowlands generally prevail, and p(T) will be the dominant factor in equation (2), leading to the usual result that frost vaporizes preferentially in lowlands.

The summer lightening of bright areas (Slipher, 1962) could be interpreted in a similar vein. However, it is not clear that such albedo increases are due to frost deposits. It seems unlikely that deposits of either H_2O or CO_2 frost are made at middle latitudes in summer near local noon when the polar caps themselves have almost completely vaporized. An explanation in terms of fine windblown dust (Sagan and Pollack, 1966) seems preferable.

4. OTHER METEOROLOGICAL EVIDENCE

Since dust storms are observed to arise in bright areas, and occasionally cover major regions of the planet, it is difficult to understand the present visibility of the dark areas, if they were lowlands (Rea, 1964); the small particles of dust should be preferentially carried by the winds into depressions. There are two additional meteorological arguments that support the characterization of the dark areas as elevations.

When a yellow cloud evolves in a bright area and is transported through the Martian atmosphere, it sometimes obscures adjacent dark areas. However, the darkest of the Martian dark areas are very rarely crossed by yellow clouds.

A striking example of this behavior is shown in Figure 2, taken from a recent publication of Dollfus (1965). These drawings were made during the 1956 opposition when a dust storm of planet-wide proportions evolved. The usual appearance of the planet in south polar projection is seen in the upper drawing, based on observations made between 5 and 18 August 1956, before the dust storm arose. The lower two drawings show the evolution and motions of yellow clouds between 19 August and 1 September 1956. The storm arose in two bright areas, Noachis on 19 August and Eridania-Electris on 25 August, and then spread. At no time in these drawings does the storm markedly cover the major adjacent dark areas, the Maria Cimmerium, Serenum, and Erythraeum; and it seems to have assiduously avoided Depressio Hellespontica, making a 180° turn around it between 24 and 26 August. Those dark areas that are covered[5] such as Mare Australe, Pandorae Fretum,

[5] Wells, 1966, describes these clouds as never transgressing the borders of the dark areas; close inspection of Figure 1 shows this to be not quite the case.

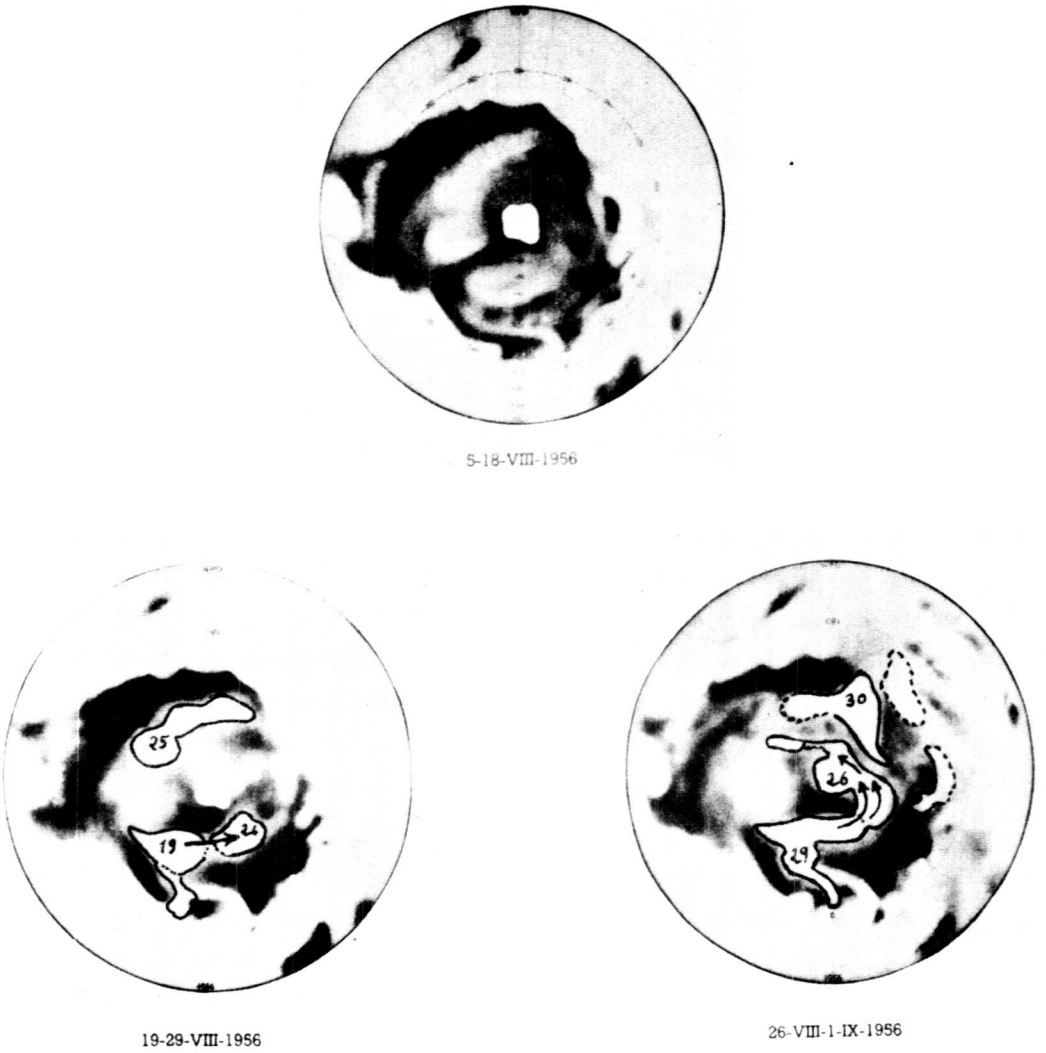

Figure 2. Evolution of the great Martian dust storm of 1956, after A. Dollfus. In this south polar projection the numbers indicate dates.

and the region of Dawes' Forked Bay in Sinus Meridiani are notable for their low contrast or narrow extent. Similar observations, including several instances of the apparent deflection of a dust cloud by a dark area, were recorded by Antoniadi (1930). The observations strongly suggest that the major dark areas constrain the possible paths of dust storms. This might be accomplished by guiding the prevailing winds along the lowlands — the northerly winds of the American Midwest are said to be guided down the Mississippi Valley and Great Plains by the Rockies on the west and the Appalachians on the east "as through a funnel" (Thompson and O'Brien, 1965). Alternatively, the dust particles will be carried only to a certain height before falling out; the particles remaining aloft will be carried by the vector component of the wind velocity along the long dimension of the depression, and the dust will appear to course through the lowlands.

Wells (1965) has attempted to interpret certain stationary condensation clouds above Martian bright areas in terms of elevation differences. These white clouds — occasionally seen in an alignment of two or three — tend to lie at the borders of dark areas, e. g., at the boundaries between Edom or Deucalionis Regio and Sinus Sabaeus. The phenomenon is attributed by Wells to a commonly observed occurrence on Earth: Air rises over a barrier whose long axis lies along the pressure gradient, adiabatically cools to the condensation point, and the condensate is then trapped in a stationary or lee wave established on the lee side of the barrier. If this explanation is correct, Wells emphasizes, it would follow that the dark areas are highlands. Because of the low water-vapor content of the Martian atmosphere, and the relatively high surface temperatures of the regions involved, the implied elevation

differences are considerable — a scale height or more. But while Wells' interpretation seems sufficient, it is not known whether it is a necessary condition for the clouds in question, and it is possible that alternative meteorological interpretations exist.

The meteorological evidence taken as a whole, however, is consistent with dark areas as elevations.

5. RADAR EVIDENCE

Confirmatory evidence that the dark areas are elevations comes from the results of radar Doppler spectroscopy of Mars (Sagan, Pollack, and Goldstein, 1966). The planet was observed at 12.5-cm wavelength with the Goldstone radar facility of the Jet Propulsion Laboratory. The quasi-specular component of the radar return resolved some 6 planetocentric degrees; the diffuse component arises from backscatter by the planet as a whole. Regions of high quasi-specular reflectivity are shown by the boxes in Figures 3 and 4 for the 1963 and 1965 oppositions, respectively. Circles denote regions at which the reflectivity reached a local maximum.

It is obvious from the figures that high radar reflectivity is associated with optical dark areas. Observations of the diurnal temperature variation (Sinton and Strong, 1960) and the photometric and polarimetric data (Dollfus, 1957) strongly suggest that both the bright and the dark areas are a powder, with the bright areas, at least, composed partly of iron oxides (Dollfus, 1957). The radar reflectivity of a planet increases with increasing bulk dielectric constant, ϵ, and with decreasing porosity of the surface layers. Iron oxides have values of ϵ in the upper range of geochemically abundant materials. If the bright areas are composed significantly of iron oxides, their low radar reflectivity implies a sizable porosity, consistent with other evidence for pulverized material in these regions. We can understand the higher radar reflectivity of the dark areas by requiring either a greater compaction of the powder in the dark areas (regardless of the dark area composition), or a smaller depth of powder in the dark

Figure 3. The 1963 radar swath superposed on Dollfus' Martian cartography (map prepared by the Space and Information Systems Division, North American Aviation). The equator and zero meridian of longitude are shown. The middle of the three parallel lines is centered at 13.°8 N. latitude, and is bounded by two lines representing the ground resolution of the quasi-specular component of the radar reflectivity. The dark rectangles represent regions of high total radar power reflectivity, and the circles represent regions of relative radar reflectivity maxima. Relevant features coded by number and by letter are as follows:

(1) Mare Acidalium
(3) Aeria
(6) Amazonis
(9) Arabia
(12) Argyre
(16) Mare Australe
(17) Baltia
(18) Mare Boreum
(28) Mare Chronium
(29) Chryse
(31) Mare Cimmerium
(38) Deucalionis Regio
(39) Deuteronilus
(42) Edom
(44) Elysium
(46) Mare Erythraeum
(51) Hellas
(52) Depressio Hellespontica
(59) Isidis Regio
(60) Ismenius Lacus
(70) Sinus Meridianii
(71) Moab
(72) Moeris Lacus
(75) Nepenthes
(77) Niliacus Lacus
(80) Nix Olympica
(85) Ortygia
(89) Pandorae Fretum
(100) Sinus Sabaeus
(104) Mare Sirenum
(109) Syrtis Major
(113) Thoth
(118) Tractus Albus
(120) Trivium Charontis
(E and F) Dawes' Forked Bay

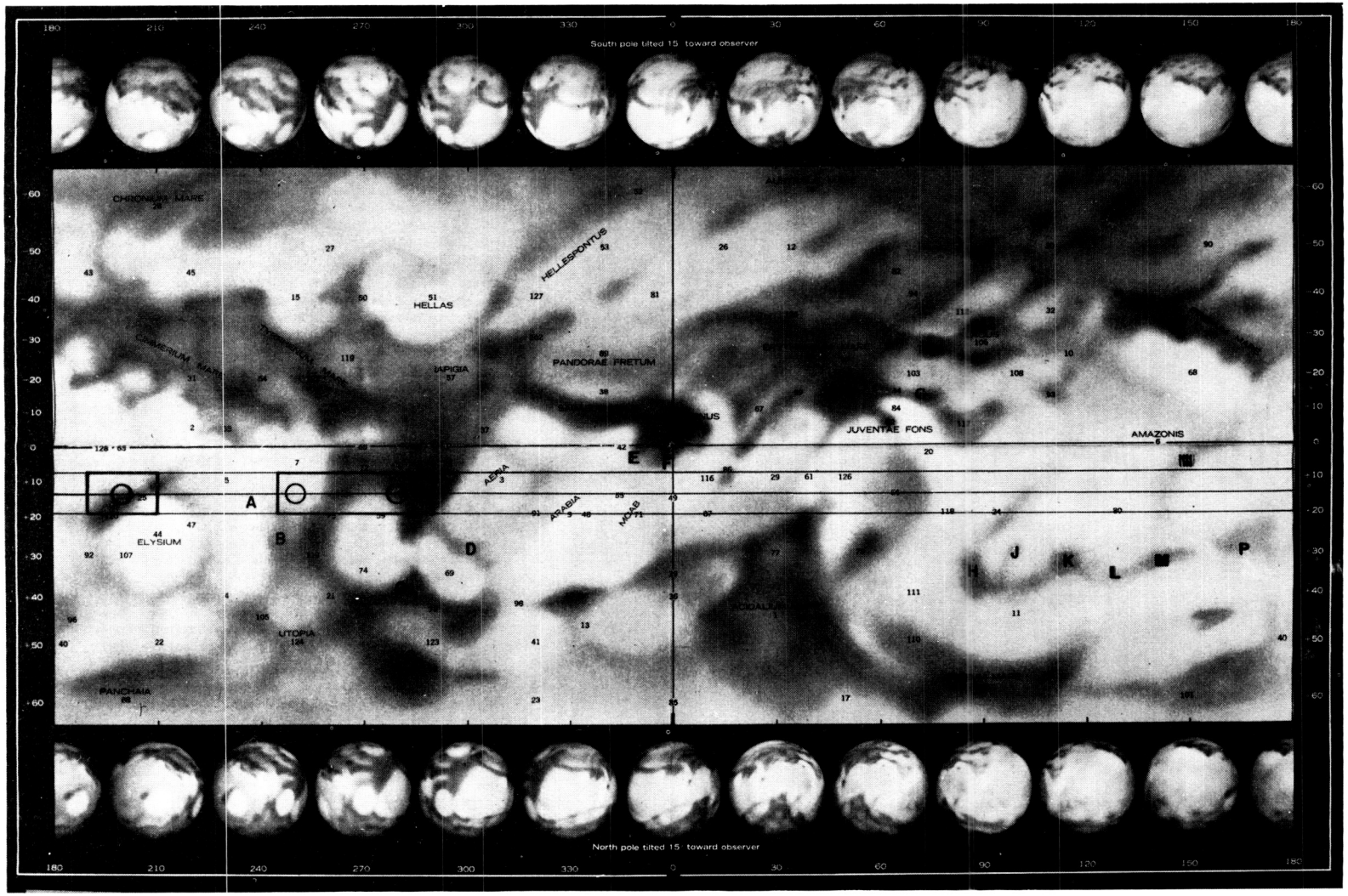
South pole tilted 15° toward observer
North pole tilted 15° toward observer
CHRONIUS LACUS
HELLESPONTUS
HELLAS
CERBERUM MARE
IAPIGIA
PANDORAE FRETUM
JUVENTAE FONS
AMAZONIS
ASPIA
ARABIA
MOAB
ELYSIUM
UTOPIA
PANCHAIA
A
B
D
E
H
J
K
L
P

Figure 4. The 1965 radar swath superposed on Dollfus' Martian cartography (map prepared by the Space and Information Systems Division, North American Aviation). The equator and zero meridian of longitude are shown. The middle of the three parallel lines is centered at 21.°6 N. latitude, and is bounded by two lines representing the ground resolution of the quasi-specular component of the radar reflectivity. The dark rectangles represent regions of high total radar power reflectivity, and the circles represent regions of relative radar reflectivity maxima. The feature code is the same as in Figure 3.

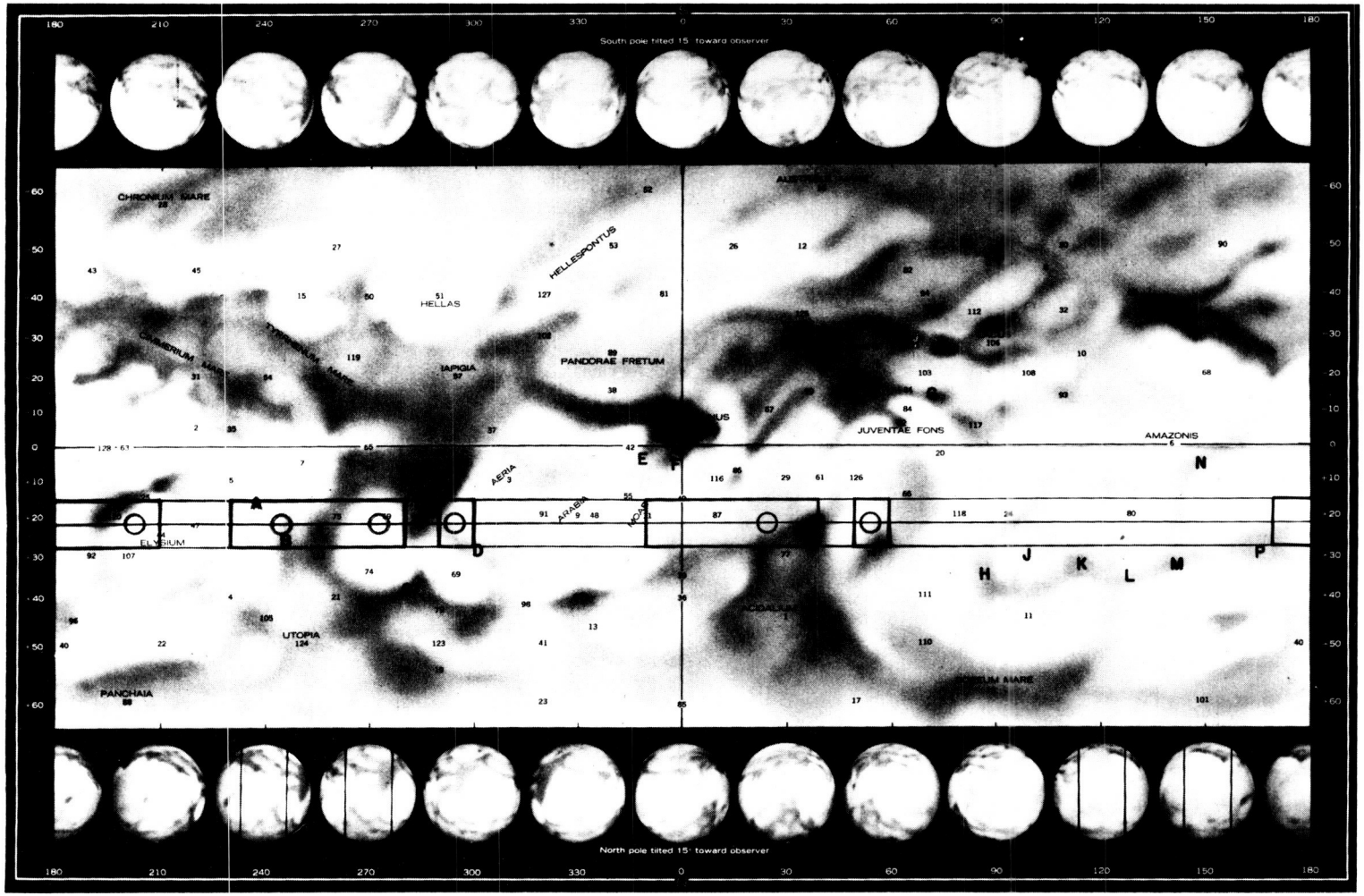
South pole tilted 15° toward observer
North pole tilted 15° toward observer
CHRONIUM MARE
HELLESPONTUS
HELLAS
PANDORAE FRETUM
IAPIGIA
AERIA
ARABIA
JUVENTAE FONS
AMAZONIS
ELYSIUM
UTOPIA
PANCHAIA
A
D
E
F
H
J
K
L
M
N
P

areas (so the radar partially sees a region of higher dielectric constant below). Either of these circumstances is plausible if the dark areas are highlands.

There is an interesting peculiarity in the radar results. From Figures 3 and 4 we see that the quasi-specular maxima are sometimes displaced by $\sim 10^\circ$ from the centroids of neighboring dark areas. While the correlation with dark areas remains excellent, this displacement is larger than the anticipated errors in the position of the subterrestrial point and in the cartography of Mars. In 1965, for example, Syrtis Major exhibits a relative reflectivity minimum but is flanked by two local maxima. These apparent anomalies can be understood by assuming a net slope for the dark areas. When the slope is under the subterrestrial point, the quasi-specular reflection will not be toward the Earth; but when the subterrestrial point is displaced from the dark area a number of planetocentric degrees approximately equal to the mean slope, a strong quasi-specular component will be detected. The geometry is illustrated in Figure 5, where we see that the near slopes of elevations, but the far slopes of depressions, will contribute. In addition, an appropriate two-dimensional alignment of a dark area in the plane of the sky will lead to an enhanced quasi-specular component. Assuming that dark areas have a general slope away from their borders with the bright areas, we expect proper alignment when normals to the dark areas (in the plane of the sky) pass through the subterrestrial point. We see from Figure 3 that the near sides of Syrtis Major and Moeris Lacus are well oriented to produce the local radar reflectivity maximum observed at 275° longitude. The far sides of these areas are less well aligned; further, the required slopes would be very steep were the far sides contributing. This conclusion is supported by similar circumstances for other regions, and especially by the contours and satellite bands of the radar Doppler spectra. For the far sides

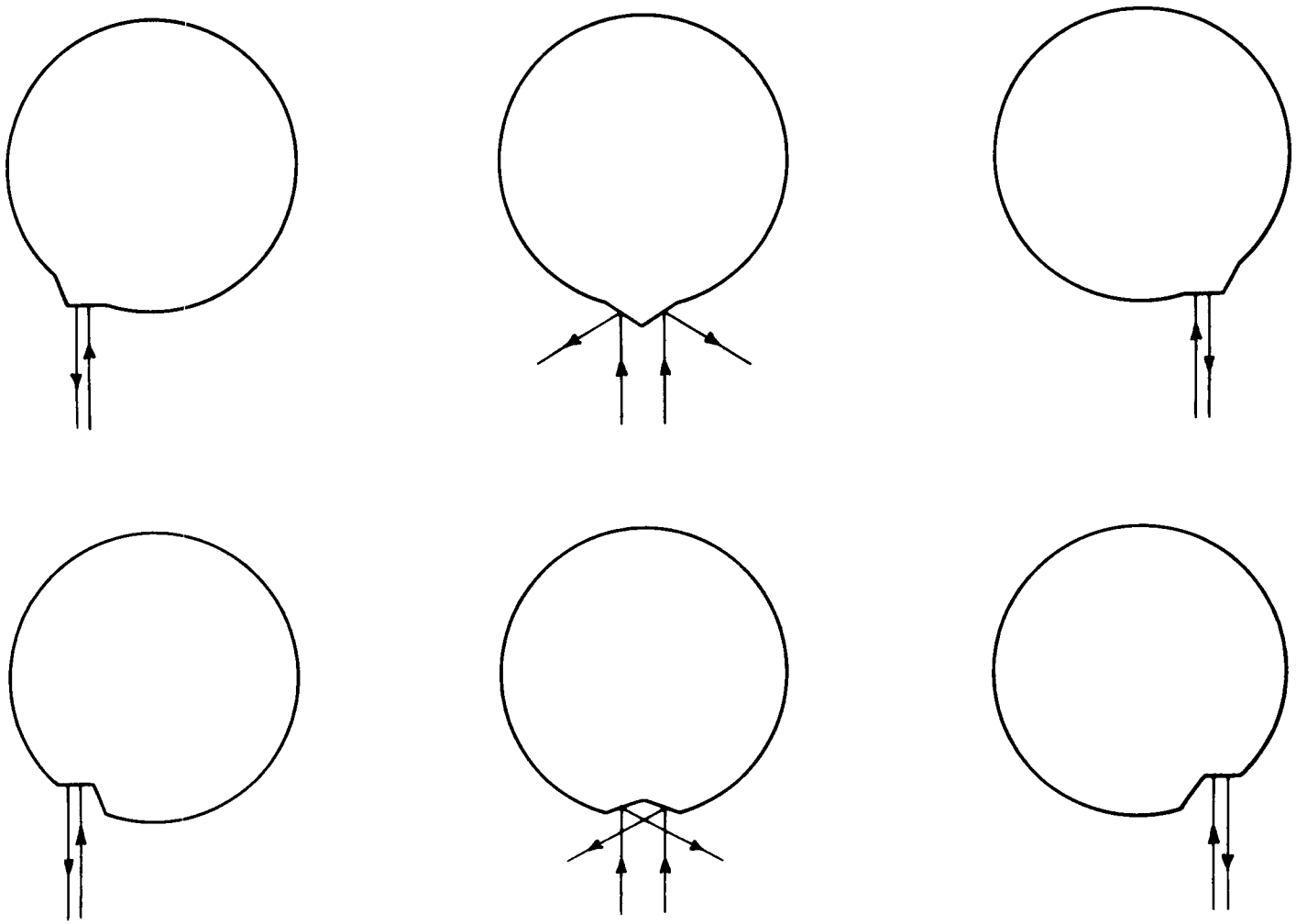

Figure 5. Diagram illustrating how both for elevations (above) and for depressions (below) a topographical feature may produce a high quasi-specular radar return when displaced from the subterrestrial point on Mars, but very weak backscattering when just under the subterrestrial point.

of dark areas to contribute, in some cases the resulting elevation differences would lead to stresses in excess of the tensile and yield strengths of ordinary materials (Sagan, Pollack, and Goldstein, 1966). We conclude that the near sides of dark areas are responsible for the displaced radar maxima, and that the dark areas are therefore highlands. The reader is referred to the original paper (Sagan, Pollack, and Goldstein, 1966) for further details.

For most of the dark areas examined in the 1965 radar swath, truncated tops are excluded by the absence of a reflection maximum in the dark area. The radar slopes and optical extents of the dark areas can then be used to compute their maximum and mean altitudes. However, a comparison of the 1963 and 1965 results (Figures 3 and 4) indicates that major dark areas such as Syrtis Major may have truncated tops. This is again consistent with arguments from the strengths of materials. The following general picture (Sagan, Pollack, and Goldstein, 1966) then emerges of the relief on the planet Mars: Some regions that characteristically exhibit prominent secular changes have very shallow slopes (1 to 2°) and ridge heights ~6 km above the adjacent deserts. Classical canals have steeper slopes (>3 to 4°) but ridge heights of the same order. Principal dark areas may have much higher altitudes, 10 to 20 km. These elevations and slopes are inconsistent neither with optical searches for elevations at the limb, nor with the tensile and yield strengths of ordinary materials under the reduced Martian gravitation. The resulting picture is similar to that expected for the Earth, were the oceans removed, the effects of water erosion eliminated, the relief amplified by the ratio of the gravitational accelerations on the two planets, and the surface then covered with fine dust. The dark areas are similar to continental blocks, and the bright areas to dry, dust-filled ocean basins.

Because of the homogeneity of Mars and its small magnetic field, as determined by Mariner 4 (Smith et al., 1965; O'Gallagher and Simpson, 1965; Van Allen et al., 1965), these conclusions bear adversely on those theories of continental origins that depend on the existence of a liquid planetary core. The elevation differences and slopes lead naturally to a quantitative inorganic model of Martian seasonal and secular changes, discussed elsewhere (Sagan and Pollack, 1966; Rea, 1964).

6. APPLICATIONS TO SURFACE PRESSURES ON MARS

The proposition that the dark areas are highlands can help explain an apparent discrepancy between the surface pressure as determined by the Mariner 4 occultation experiment and as determined by recent infrared spectrometric observations. Immersion occurred (Kliore, Cain, and Levy, 1966) at a latitude of 50°.5 S.[6] and a longitude 183° W. and the differential refraction observed implied (Kliore et al., 1965) a surface pressure of 4.9 ± 0.8 mb if the atmosphere is composed only of CO_2, and 6.0 ± 1.0 mb for an atmosphere composed of 50% CO_2 and 50% N_2 and Ar.

An occultation measurement of pressure is necessarily biased toward high elevations. Consider a highland of elevation, h, above the mean surface, and also a line of sight tangent both to the elevation and, at point O, to the mean sphere (see Figure 6). If the elevation is a horizontal distance x_{max} or less from O, the line of sight will intercept the elevation rather than the mean sphere. We readily find that

$$x_{max} \simeq (2 R_{\sigma} h)^{1/2} \quad , \tag{3}$$

provided $h \ll 2 R_{\sigma}$, where R_{σ} is the planetary radius, 3.3×10^3 km. When h = 10 km, x_{max} = 250 km. The effective height, h_{eff}, above point O intercepted by the line of sight when $x \leq x_{max}$ is

[6] A misprint in the original announcement (Kliore et al., 1965) put this latitude at 55° S.

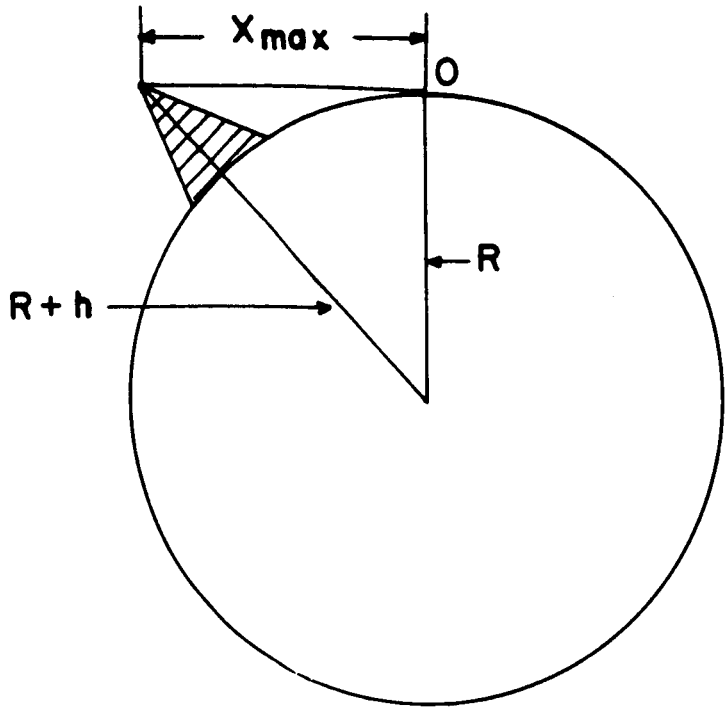

Figure 6a.

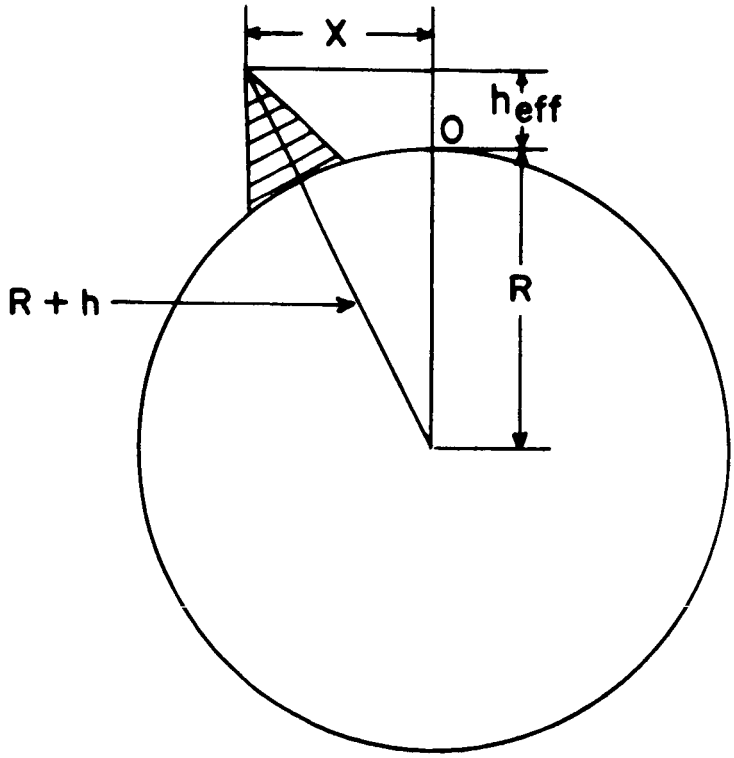

Figure 6b.

Figure 6. Occultation geometry in the vicinity of an elevation.

$$h_{eff} = h\left(1 - x^2/x^2_{max}\right) = h - \left(x^2/2R_{\sigma}\right) \quad . \tag{4}$$

When $x = x_{max}/2$, $h_{eff} = 3h/4$. Thus, if elevations of the order discussed above lie within about 150 km of the nominal occultation tangent, O, and along the line of sight, the Mariner 4 pressures will refer to some significant fraction of a scale height above the mean surface. The actual surface pressures will be a factor $\sim$ 2 higher, assuming the Mariner 4 occultation scale height of 9 $\pm$ 1 km (Kliore et al., 1965).

The immersion nominal surface tangent is shown in Figure 7; it is within three planetocentric degrees of an extension of Mare Chronium. The canal Ascanius (Antoniadi, 1930) is also nearby. Thus, since the immersion nominal tangent lies, within the errors of Martian cartography, a few hundred kilometers from both bright and dark areas, the occultation pressure will be anomalously low, regardless of whether bright areas or dark areas are highlands.

The emersion nominal surface tangent is shown in Figure 8; it intercepts Mars at 60° N. latitude, 34° W. longitude. While this locale has been described (Kliore, Cain, and Levy, 1966) as in Mare Acidalium, inspection of Figure 8 — based on the 1965 visual observations by Focas (1966) — reveals that the tangent lies within a bright area, a pass connecting the Ortygia and Baltia deserts. Thus, within the cartographic errors (approximately a few degrees) emersion seems to have occurred in a bright area adjacent to dark areas. Again the occultation pressures must be biased toward low values. Note that relative to the mean spheroid of Mars it is entirely possible that immersion occurred over higher elevations than emersion.

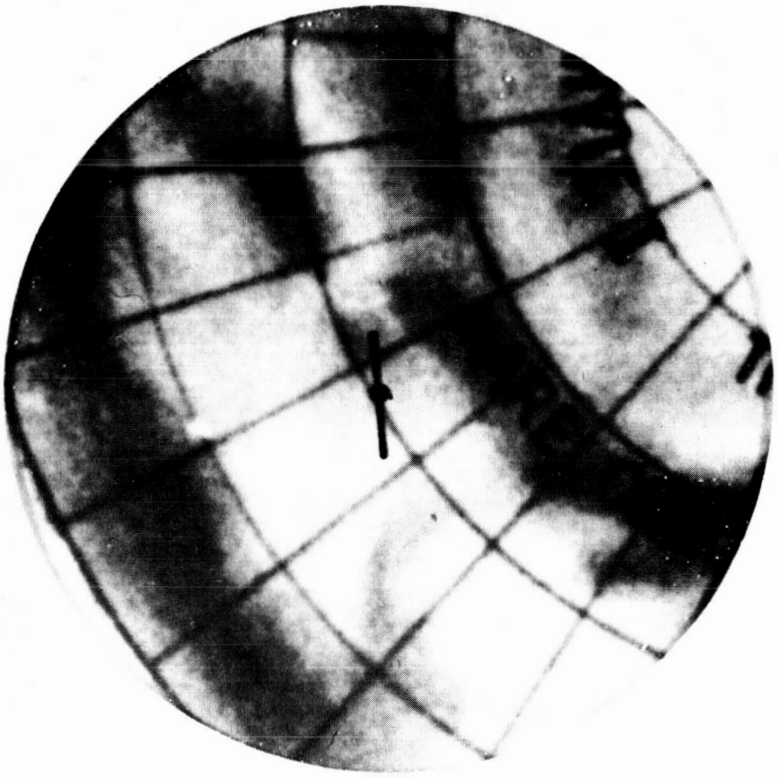

Figure 7. Position of the immersion nominal tangent of the Mariner 4 occultation experiment on the surface of Mars. The position of the tangent is shown by the dot and the direction of the spacecraft-to-earth line of sight is shown by the line, 300 km long. The nearest major dark area in this south polar projection of the International Astronomical Union Mars cartography is Mare Chronium.

Figure 8. Position of the emersion nominal tangent of the Mariner 4 occultation experiment on the surface of Mars. The position of the tangent is shown by the dot and the direction of the spacecraft-to-earth line of sight is shown by the line, 300 km long. In this 1965 map of Mars prepared by Dr. J. H. Focas the tangent lies in a channel through the major dark area Mare Acidalium.

The emersion pressure is 8.4 ± 1.3 mb for pure CO_2 (Kliore, Cain, and Levy, 1966) and about 9 ± 1.3 mb for 50% CO_2 and 50% N_2 and Ar. The difference between emersion and immersion pressures is then 3 to 3.5 mb, larger than the maximum combined errors. The difference is, however, small enough to be accounted for easily by differences in local relief along the nominal surface tangents, regardless of whether bright areas or dark areas are highlands. A barely significant difference was recorded between the effective planetary radii at immersion and emersion (Kliore, Cain, and Levy, 1966); however, as the experimenters themselves point out, when allowance is made for the oblateness of Mars (immersion and emersion occurred at different latitudes), no significant altitude difference remains. The altitude difference corresponding to the observed pressure difference lies within the probable error of measurement.

The most recent ground-based technique for determining Martian surface pressure has been curve-of-growth analysis of near-infrared CO_2 bands (see, e.g., Chamberlain and Hunten, 1965; Cann et al., 1965). The CO_2 abundance can be determined from a weak-line band, and the product of abundance and total pressure from a strong-line band. Prior to the 1965 opposition a variety of spectrometric observations led to surface pressures ranging between 13 and 33 mb (see Cann et al., 1965). Subsequent to the announcement of the occultation pressures, data from the 1965 opposition have been reduced. These results are remarkably uniform (see, e.g., the results discussed in Brown et al., 1966), yielding surface pressures 10^{+10}_{-5} mb, which are consistent with the immersion occultation pressures only by stretching the probable errors.

The spectrometric pressure determinations generally refer to some average of the bright and dark areas intercepted by the slit. We have already seen that the occultation results are biased toward the pressures at elevations. We hypothesize that the difference between occultation and spectrometric pressures is attributable to this cause.

The globes at the bottoms of Figures 3 and 4 show the appearance of Mars when the subterrestrial point lies at Martian latitude 15° N. At the 1963 opposition the subterrestrial point lay at 13°.8; at 1965, 21°.6. During the 1963 opposition, there was a vast predominance of bright areas on the disk of Mars — on the average about 75% of the area of the disk, and occasionally (see right-hand globes) as much as 90%. At no other opposition is this proportion larger. During the 1965 opposition, owing to the increased prominence of the Maria Acidalium and Boreum, and the north polar dark areas, the proportion of bright areas was often less. If the bright areas are lowlands, some of the difference between the pre-1965 and post-1965 spectrometric results may be due to the relative configuration of markings on the planetary disk during the observing periods.

The mean pressures in bright and dark areas will now be estimated. The spectrometric pressure, $\overline{P}$, a mean over bright and dark areas, can be written for the 1963 and 1965 oppositions as

$$\overline{P} \simeq 0.75\ P_b + 0.25\ P_d \quad , \tag{5}$$

where P_b and P_d are, respectively, the mean pressures of the bright and dark areas. A conservative average for these two oppositions is $\overline{P} \simeq 12$ mb. From the occultation measurements, a typical highland

pressure (both immersion and emersion were in border areas) is 6 mb. Adopting our thesis that dark areas are highlands, we find

$$P_d \simeq 6 \text{ mb}$$
$$P_b \simeq 14 \text{ mb} \quad . \tag{6}$$

These are mean pressures for dark and bright areas. Assuming a 9-km scale height, the corresponding altitude difference is about 8 km, in good agreement with the radar results.

If the bright areas are as deep as the dark areas are high, their lowest reaches should be another 4 km below the mean level of the bright areas. The corresponding pressures – presumably at the centers of extended bright areas – are 22 mb. The elevation difference between the highest elevations and the lowest depressions would then be 16 km, consistent with yield and tensile strength restraints. Had we weighted the 1963 spectrometric pressures at all, greater altitude differences would result. Because the bright areas are intrinsically less reflective to radar than are the dark areas, a continuing downward slope in the bright areas away from the dark-area boundaries – as in terrestrial ocean basins – is not excluded by the radar data. Since the bright areas have greater extent than the dark areas on Mars, gentler slopes will achieve the same elevation differences.

More reliable recent polarization measurements support this conclusion. From Dollfus' new data, it can be shown that the contribution of atmospheric particulate matter to polarization in the visible is small; the resulting surface pressures near the center of a bright area are 16 mb for a pure CO_2 atmosphere, 19 mb for an atmosphere 50% CO_2 and 50% N_2, and 25 mb for a pure N_2 atmosphere (Pollack, 1966).

The possibility of pressures in excess of 15 mb at certain locales on Mars is of substantial interest to designers of spacecraft intended for soft landings. For Saturn 1B-Centaur or Titan 3C class missions, with ballistic entry and parachutes for achieving low terminal velocities, the density of the Martian atmosphere has a critical influence on the allowable scientific payload. In the vicinity of 10-mb surface pressure a virtual discontinuity occurs in the useful aerodynamic drag (see, e.g., Levinthal, 1966); and below 6 mb the allowable scientific payload vanishes. In the 15- to 20-mb range, on the other hand, from 20 to 50% of the entry mass is utilizable for science with terminal velocities between 30 and 80 ft/sec (Levinthal, 1966). These considerations suggest that the sites for soft landing on Mars most favorable from an engineering standpoint are the centers of major bright areas relatively uncontaminated by dark areas — e.g., Elysium, Hellas, Arabia, and Tractus Albus. This suggestion is at variance with previous landing-site recommendations (Swan and Sagan, 1965) based on scientific interest in the dark areas.

7. THE OBLATENESS OF MARS

It has been recognized for some time that the dynamical oblateness of Mars, as measured by the advance of the line of apsides of the Martian satellites, Phobos and Deimos, is inconsistent with the optical oblateness, as measured with filar and double-image micrometers and also photographically. The dynamical oblateness is 0.0052, while a recent weighted mean of the optical oblateness is 0.0105 ± 0.0005 (de Vaucouleurs, 1964). The optical oblateness corresponds to a difference between equatorial and polar radii of 36 km; only about half of this is accounted for by the dynamical oblateness.

With 10-mb mean surface pressure and a Rayleigh scattering atmosphere it is easy to show that, at the limb, the brightness of scattered light in the yellow from atmospheric regions several scale heights up is comparable to the surface brightness of the planet. Since we expect the equatorial scale height to exceed the polar scale height, the optical oblateness measured in the usual way can be attributed almost entirely to such atmospheric effects. However, a separate measure of the oblateness of Mars was made by Trumpler (1927), who followed photographically the paths demarcated by Martian surface features over the disk as the planet rotates. The oblateness determined by this method, which is essentially independent of atmospheric scattering, is 0.0108, coincidentally in good agreement with the results of other optical techniques. Trumpler's oblateness refers then to the actual figure of the planetary surface, and the discrepancy of his result with the dynamical oblateness must be explained.

A remarkable suggestion has been advanced by Urey (1950, 1952): "If continental blocks exist in the equatorial regions and not at the poles,

and if hydrostatic equilibrium obtains, an equatorial bulge would be produced which would appear [in measurements of the optical oblateness] but would be undetected by the moons' motions," because the moons recognize only the mean oblate spheroid. (Also optical diameter measurements suffer the same bias to peaks that the occultation experiment does.) Urey then went on to reject the hypothesis in the following terms: "But... such high plateaus or mountains (some 15 km high) even in the tropical regions should be covered by snow as on earth, and such regions are not observed. Also, the seasonal changes in color in the tropics so suggestive of plant life argue against such high regions."

We have seen, however, in the early parts of the present discussion that elevations are not expected to be sensibly cooler than depressions on Mars. The dark areas of Mars tend to concentrate near equatorial latitudes (see Figures 3 and 4), and elevation differences between major dark and bright areas in the 10- to 15-km range have been deduced from several lines of evidence. While the entire effect may not be due to equatorial elevations, and while there are other significant influences on the figure of Mars, we believe that Urey's explanation of the discrepancy between dynamical and optical oblateness now has some measure of observational support.

8. APPLICATIONS TO LIFE ON MARS

The foregoing results may have some relevance to the possibility of life on Mars. Conceivable advantages of the dark areas as habitats are their slightly higher daytime temperatures (~8 C°), and the diminished probability of burial by drifting dust. On the other hand, if bright areas are lowlands, more water will precipitate out at night (because of the increased pressure for a constant mixing ratio); and the precipitated water would survive daytime vaporization longer, because of the lower mean wind velocity in the lowlands.

Perhaps the most important biological difference between bright areas and dark areas concerns the stability field of liquid water. The triple-point pressure of water is just under 6 mb. If, as the occultation data suggest, 6 mb is a typical dark area pressure, liquid water may be generally unavailable in Martian dark areas. In bright areas on the borders of dark areas the liquid range of water is 0° to about 13° C. For bright areas near the equator, this temperature range is experienced for about 1 hour, twice a day (Sinton and Strong, 1960). In the centers of bright areas, where $P \simeq 20$ mb, the liquid range is 0° to about 18° C and for equatorial regions occurs for somewhat under 2 hours, twice a day. Thus Martian surface biology based on aqueous biochemistries seems much more likely in bright areas than in dark. Since they also seem much more accessible for soft landings, the centers of extensive Martian bright areas are the preferred sites for in situ biological investigations of Mars.

9. SUMMARY

Observations of apparent frost phenomena occurring preferentially in the Martian bright areas has, in the past, led to the conclusion that the bright areas are elevations. The argument hinges on the assumption that near midday highlands should be colder than lowlands. On the Earth this assumption is valid because the highlands experience (1) diminished greenhouse effect, (2) a greater inclination of surfaces to the Sun's rays, and (3) turbulent mixing and radiation exchange between the surface and adiabatically cooled rising air. Because of the lower pressure and more shallow slopes on Mars, these factors together cool the highlands by at most a few K° . Contrary to the conclusions previously drawn, the polar cap recession data suggest the dark areas are highlands, because of the greater wind velocities and frost-vaporization rates anticipated for highlands. A variety of meteorological observations support this conclusion.

From the quasi-specular component of the radar power reflectivity, and from the radar Doppler spectra, both as a function of Martian longitude, the Martian dark areas are found to have systematically higher elevations than the adjacent bright areas. Mean slopes of a few degrees are deduced, and elevation differences up to 17 km are inferred. These slopes and elevation differences are similar to those expected for the Earth if oceans and water erosion were removed, and relief amplified by the ratios of the gravitational accelerations on the two planets. These elevation differences are consistent with the yield and tensile strengths of common materials, and with unsuccessful searches for elevations at the Martian terminator. The concentration of dark highlands near the Martian equator may help explain the discrepancy between the dynamical and the optical oblateness of Mars.

The results bear on the discrepancy between ground-based infrared spectrometric and Mariner 4 occultation values of Martian surface pressures. The infrared pressures (~12 mb) refer to an average over bright and dark areas. The occultation pressures (~6 mb) are necessarily biased toward elevations; both ingress and egress occurred in or very near dark areas. Taking the occultation pressures as typical of highlands, predicted pressures in the centers of prominent bright areas are ~20 mb, permitting parachute landings of relatively modest spacecraft at these locales. The higher pressures deduced for bright areas make them the preferred locales for liquid water on Mars (for a few hours a day), and therefore the preferred sites for living systems based on aqueous biochemistries.

10. ACKNOWLEDGMENTS

We wish to acknowledge helpful discussion with or communication from M. J. S. Belton, F. D. Drake, A. Dollfus, V. R. Eshleman, J. H. Focas, P. Gierash, R. M. Goody, T. C. Owen, I. I. Shapiro, H. Spinrad, and R. A. Wells.

11. REFERENCES

ANTONIADI, E. M.

1930. La Planète Mars. Hermann, Paris, 239 pp.

BROWN, H., STANLEY, G. J., MUHLEMAN, D. O., AND MÜNCH, G., eds.

1966. Proc. Caltech – JPL Lunar and Planetary Conf. (JPL Tech Memo 33-206), Pasadena, California, 307 pp.

CANN, M. W. P., DAVIES, W. D., GREENSPAN, J. A., AND OWEN, T. C.

1965. A review of recent determinations of the composition and surface pressure of the atmosphere of Mars. NASA Contractor Rep. CR-298, 186 pp.

CHAMBERLAIN, J. W., AND HUNTEN, D. M.

1965. Pressure and CO_2 content of the Martian atmosphere – a critical discussion. Revs. Geophys., vol. 3, pp. 299-317.

DENT, W. A., KLEIN, M. J., AND ALLER, H. D.

1965. Measurements of Mars at λ3.75 cm from February to June, 1965. Astrophys. Journ., vol. 142, pp. 1685-1688.

DOLLFUS, A.

1957. Étude des planètes par la polarization de leur lumière. Ann. d'Astrophys. Suppl. No. 4, 114 pp.

1961. Visual and photographic studies of planets at the Pic du Midi. In Planets and Satellites (vol. 3 of The Solar System), ed. by G. P. Kuiper and B. M. Middlehurst, Univ. of Chicago Press, Chicago, pp. 534-571.

1965. Étude de la planète Mars de 1954 à 1958. Ann. d'Astrophys., vol. 28, pp. 722-747.

FOCAS, J. H.

1966. Private communication.

GOODY, R. M.

1964. Radiative transfer and fluid motions. In Atmospheric Radiation. I. Theoretical basis. Clarendon Press, Oxford, pp. 344-370.

1966. Private communication.

GOODY, R. M., AND BELTON, M. J. S.

1966. Radiative relaxation times for Mars: A discussion of Martian atmospheric dynamics, Planet. and Space Sci., in press.

HOWARD, J. N., BURCH, D. L., AND WILLIAMS, D.

1955. Infrared transmission through synthetic atmospheres. Geophys. Res. Paper No. 40, Geophys. Res. Dir., Air Force Cambridge Res. Center, Bedford, Mass., 244 pp.

KLIORE, A., CAIN, D. L., AND LEVY, G. S.

1966. Radio occultation measurement of the Martian atmosphere over two regions by the Mariner IV space probe. Paper presented at the 7th Intl. Space Sci. Symp., Vienna, 18 pp., to be published.

KLIORE, A., CAIN, D. L., LEVY, G. S., ESHLEMAN, V. R., FJELDBO, G., AND DRAKE, F. D.

1965. Occultation experiment — results of the first direct measurement of Mars's atmosphere and ionosphere. Science, vol. 149, pp. 1243-1248.

KUIPER, G. P.

1957. Visual observations of Mars. Astrophys. Journ., vol. 125, pp. 307-317.

LEIGHTON, R. B., AND MURRAY, B. C.

1966. Behavior of carbon dioxide and other volatiles on Mars. Science, vol. 153, pp. 136-144.

LEVINTHAL, E. C.

1966. Space vehicles for planetary missions. In Biology and the Exploration of Mars, ed. by C. S. Pittendrigh, W. Vishniac, and J. P. Pearman, Publ. 1296, Natl. Acad. Sci., Natl. Res. Council, Washington, D.C., pp. 292-322.

LOWELL, P.

1906. Mars and Its Canals. Macmillan, New York, 393 pp.

1908. Mars as the Abode of Life. Macmillan, New York, 288 pp.

O'GALLAGHER, J. J., AND SIMPSON, J. A.

1965. Search for trapped electrons and a magnetic moment at Mars by Mariner IV. Science, vol. 149, pp. 1233-1239.

OHRING, G., WEN TANG, AND DE SANTO, G.

1962. Theoretical estimates of the average surface temperature on Mars. Journ. Atmos. Sci., vol. 19, pp. 444-449.

POLLACK, J. B.

1966. Rayleigh scattering in an optically thin atmosphere and its application to Martian topography. Icarus, in press.

REA, D. G.

1964. The darkening wave on Mars. Nature, vol. 201, pp. 1014-1015.

RUSSELL, H. N., DUGAN, R. S., AND STEWART, J. Q.

1945. Astronomy. I. The Solar System. Rev. ed., Ginn and Co., Boston, pp. 331-332.

SAGAN, C.

1961. The abundance of water vapor on Mars. Astron. Journ., vol. 66, pp. 52-53.

1966. The solar system as an abode of life. In Biology and the Exploration of Mars, ed. by C. S. Pittendrigh, W. Vishniac, and J. P. Pearman, Publ. 1296, Natl. Acad. Sci., Natl. Res. Council, Washington, D.C., pp. 73-113.

SAGAN, C., AND POLLACK, J. B.

1966. An inorganic model of Martian phenomena. Astron. Journ., vol. 71, p. 178, and to be published.

SAGAN, C., POLLACK, J. B., AND GOLDSTEIN, R. M.

1966. Radar Doppler spectroscopy of Mars. Smithsonian Astrophys. Obs. Spec. Rep. No. 221

SCHORN, R., et al.

1966. Astrophys. Journ., in press.

SINTON, W. M., AND STRONG, J.

1960. Radiometric observations of Mars. Astrophys. Journ., vol. 131, pp. 459-469.

SLIPHER, E. C.

1962. The Photographic Story of Mars. Sky Publ. Corp., Cambridge, Mass., 168 pp.

SMITH, E. J., DAVIS, L., JR., COLEMAN, P. J., JR., AND JONES, D. E.

1965. Magnetic field measurements near Mars. Science, vol. 149, pp. 1241-1242.

SWAN, P. R., AND SAGAN, C.

1965. Martian landing sites for the Voyager mission. Journ. Spacecraft and Rockets, vol. 2, pp. 18-25.

THOMPSON, P. D., AND O'BRIEN, R.

1965. Weather, Time Inc., New York, p. 15.

TOMBAUGH, C.

1961. The Atmospheres of Mars and Venus, ed. by W. W. Kellogg and C. Sagan, Publ. 944, Natl. Acad. Sci., Natl. Res. Council, Washington, D.C., pp. 66-67.

1966. The absence of an aqueous morphology on Mars and some geologic consequences. Icarus, in press.

TROUVELOT, E.-L.

1884. Observations sur la planète Mars. Compt. Rend., vol. 98, p. 789.

TRUMPLER, R. J.

1927. Observations of Mars at the opposition of 1924. Lick Obs. Bull. No. 13, Univ. of Calif. Press, Berkeley, p. 19.

UREY, H. C.

1950. The structure and chemical composition of Mars. Phys. Rev., vol. 80, p. 295.

1952. The Planets: Their Origin and Development. Yale Univ. Press, New Haven, Conn., 245 pp.

VAN ALLEN, J. A., FRANK, L. A., KRIMIGIS, S. M., AND HILLS, H. K.

1965. Absence of Martian radiation belts and implications thereof. Science, vol. 149, pp. 1228-1233.

DE VAUCOULEURS, G.

1964. Geometric and photometric parameters of the terrestrial planets. Icarus, vol. 3, pp. 187-235.

WELLS, R. A.

1965. Evidence that the dark areas on Mars are elevated mountain ranges. Nature, vol. 207, pp. 735-736.

1966. ESRO Scientific Note SN-54.

APPENDIX A

DIFFERENTIAL GREENHOUSE EFFECT BETWEEN HIGHLANDS AND LOWLANDS

We wish to calculate roughly the temperature difference, ΔT, between highland and lowland due to the differential greenhouse effect on Mars. Radiation balance at the surface gives

$$T_e^4 + (1 - f)\, T_A^4 = T_s^4 \quad , \qquad \text{(A-1)}$$

when T_e is the effective planetary temperature (calculated from the solar constant and Martian bolometric albedo), T_A is the radiation temperature of the atmosphere, and T_s is the surface temperature. The fraction of the surface emission to space that falls in window regions is f. Since $T_A \simeq T_s \equiv T_e + \Delta T$, Taylor series expansion of equation (A-1) gives $\Delta T \propto (1 - f)$. Because of the low water vapor abundance and low surface pressure on Mars, the infrared atmospheric opacity is governed by the 15-μ CO_2 band. The equivalent width of this band $\int A_\nu (15\,\mu)\, d\nu$ is then $\propto (1 - f) \propto \Delta T$. The dependence of $\int A_\nu (15\mu)\, d\nu$ on pressure and CO_2 abundance is discussed by Howard, Burch, and Williams (1955). Scaling from the greenhouse results of Ohring, Wen Tang, and DeSanto (1962) to contemporary values of $P \simeq 10$ mb, and $w_{CO_2} \simeq 60$ m-atm, we derive a value of $\Delta T \simeq 8.5$ K°. The differential greenhouse effect between elevations and depressions with an atmospheric pressure difference of a factor 2 is then $\simeq 1.3$ K°, consistent with our expectation from the microwave observations.

APPENDIX B

COOLING OF MARTIAN HIGHLANDS BY RISING AIR

We wish to compute the cooling of highlands on Mars due to energy exchange between the highlands and adiabatically cooled parcels of rising air. This energy exchange is due to turbulent mixing and radiation, both when there is a prevailing wind and when there is not.

Consider a parcel of air rising over an elevation (a mountain range, say, or a continental block), as shown in Figure 1. The wind velocity, v, carries the parcels along the streamlines, as illustrated. The rate of heat loss, dh/dt, per unit area of elevation, in heating the overlying atmosphere, equals the heat gained by those parcels of air above the elevation, divided by the time these parcels spend over the elevation:

$$\frac{dh}{dt} = c_p(T_e - T_a)\,\beta\,\rho_0\,\frac{D}{t} \quad . \tag{B-1}$$

The factor $c_p(T_e - T_a)$ is the heat gained in the energy exchange by a unit mass of atmosphere; c_p is the specific heat at constant pressure; and $T_e - T_a$ is the mean temperature difference between an average locale on the elevation and the adjacent air — cooled due to adiabatic expansion up the slopes of the elevation. The factor $\beta\,\rho_0\,D$ is the total mass of atmosphere above the elevation (for moderate slopes) which participates in the heat exchange. The thickness of the boundary layer that participates in the exchange during the characteristic time of the problem is D, and the density of air near the ground, ρ_0. The

fraction of the atmosphere above the elevation that at any given time participates in adiabatic expansion and moves across (rather than along) the elevation is β.

The characteristic time of the problem is t. In the case of forced convection at prevailing velocity, v, up a slope of slant length a, $t = 2a/v$. In the case of free convection, t is the time scale for efficient radiative and conductive exchange between the surface and the boundary layer. Approximately for, both cases, $D \propto t$. On Mars the principal radiative exchange between atmosphere and surface is in the 15-μ CO_2 band; the solution of the corresponding radiative relaxation time problem leads to a proportionality constant between D and t of the order unity in cgs units for a pure CO_2 atmosphere at 3-mb pressure (Goody and Belton, 1966). (Calculation of D/t can be made from the relations found in Goody (1964).) For more probable Martian CO_2 abundances and total pressures, this constant is closer to 1/2. Thus, equation (B-1) may be rewritten as

$$\frac{dh}{dt} = \frac{1}{2} c_p (T_e - T_a) \beta \rho_0 \quad \text{(cgs)}$$

and the rate of heat exchange is seen to vary as ρ_0.

The value of c_p is approximately 0.2 cal $gm^{-1}(K°)^{-1}$ for a mixture of CO_2 and N_2 at Martian temperatures and pressures, and is very insensitive to changes in any of these parameters. If we take the pressure halfway up the elevation to be 10 mb (see discussion of pressures above), then $\rho_0 \simeq 2 \times 10^{-5}$ gm cm^{-3}.

The maximum elevation difference that can be supported on Mars is $\sim$ 25 km (Sagan, Pollack, and Goldstein, 1966). If we take half

this as an upper limit to the mean elevation differences, and the standard dry adiabatic lapse rate for Mars of $-3.7\ K^\circ\ km^{-1}$, we find that the air at the altitude of elevations will (in the absence of the elevation) be at most some 50 K° cooler than the air at the altitude of depressions. The upper limit to $T_e - T_a$ is then $\simeq$ 50 K°. Parcels beginning at higher elevations have less steep streamlines (see Figure 1), and consequently experience less adiabatic cooling on rising. Not all the atmosphere overlying the elevation will participate in the flow, and the prevailing winds will not flow all the time. Thus, $10^\circ K \leq \beta (T_e - T_a) \leq 50\ K^\circ$.

With the above numbers, we find

$$2\times10^{-5}\ \text{cal cm}^{-2}\ \text{sec}^{-1} \leq \frac{dh}{dt} \leq 1 \times 10^{-4}\ \text{cal cm}^{-2}\ \text{sec}^{-1}\ . \quad \text{(B-2)}$$

We can compare this heat exchange between atmosphere and elevation with S, the energy absorbed by an area with the Martian bolometric albedo $\simeq$ 0.3 (de Vaucouleurs, 1964) when the sun is directly overhead: $S \simeq 10^{-2}\ \text{cal cm}^{-2}\ \text{sec}^{-1}$. The temperature change ΔT that results is, through the Stefan-Boltzmann law, given by $(T - \Delta T)^4 \simeq T^4 - (S^{-1}\, dh/dt)\, T^4$, where $T \sim 200^\circ$ K is a typical Martian surface temperature. Thus,

$$\Delta T \simeq \frac{1}{4}\,(dh/dt)\,(T/S) \quad , \qquad \text{(B-3)}$$

and, from equation (B-2),

$$0.1\ K^\circ \leq \Delta T \leq 0.5\ K^\circ \qquad \text{(B-4)}$$

for Mars. On the earth, ΔT can be sizable, because ρ_0 is so much larger.

These calculations of cooling due to adiabatic expansion and heat exchange have assumed a zero solar zenith angle. For other solar elevations, $S \propto \cos \theta$, where θ is the angle between the line of sight to the sun and the local planetary normal. Thus, throughout most of the day the influence of $\cos \theta$ on ΔT is a factor ~ 2. As night approaches, the conductive flux from the subsurface will establish a surface temperature of 150 to 200° K (Sinton and Strong, 1960) corresponding to a flux $\sim 10^{-3}$ cal $cm^{-2} sec^{-1}$. While atmospheric heat exchange becomes relatively more important at night, the nighttime temperature regimes are dominated by the thermal inertia and not by heat exchange with the atmosphere.

NOTICE

This series of Special Reports was instituted under the supervision of Dr. F. L. Whipple, Director of the Astrophysical Observatory of the Smithsonian Institution, shortly after the launching of the first artificial earth satellite on October 4, 1957. Contributions come from the Staff of the Observatory.

First issued to ensure the immediate dissemination of data for satellite tracking, the reports have continued to provide a rapid distribution of catalogs of satellite observations, orbital information, and preliminary results of data analyses prior to formal publication in the appropriate journals. The Reports are also used extensively for the rapid publication of preliminary or special results in other fields of astrophysics.

The Reports are regularly distributed to all institutions participating in the U. S. space research program and to individual scientists who request them from the Publications Division, Distribution Section, Smithsonian Astrophysical Observatory, Cambridge, Massachusetts 02138.